

Atomic density of a harmonically trapped ideal gas near Bose-Einstein transition temperature

R. Hoppeler¹, J. Viana Gomes^{1 a}, and D. Boiron¹

Laboratoire Charles Fabry de l'Institut d'Optique,
UMR 8501 du CNRS, F-91403 Orsay Cedex, France

Received: date / Revised version: date

Abstract. We have studied the atomic density of a cloud confined in an isotropic harmonic trap at the vicinity of the Bose-Einstein transition temperature. We show that, for a non-interacting gas and near this temperature, the ground-state density has the same order of magnitude as the excited states density at the centre of the trap. This holds in a range of temperatures where the ground-state population is negligible compared to the total atom number. We compare the exact calculations, available in a harmonic trap, to semi-classical approximations. We show that these latter should include the ground-state contribution to be accurate.

PACS. 03.75.Hh Static properties of condensates; thermodynamical, statistical and structural properties – 03.65.Sq Semiclassical theories and applications – 05.30.Jp Boson systems

The phenomenon of Bose-Einstein condensation (BEC) is a phase transition. Below the critical temperature T_c , the ground-state population, which is the order parameter, becomes macroscopic. This phenomenon, that happens strictly speaking only at the thermodynamic limit, is usually illustrated in textbooks with a homogeneous gas. Experimentally, the Bose-Einstein condensation of dilute gases has been observed since 1995 with atoms confined in a harmonic trap [1]. These stimulating experimental data have quickly pointed out that two effects had to be taken into account: the interatomic interactions and the finite number of atoms [2]. Several papers, as the present one, have studied harmonically trapped ideal gases containing a finite number of atoms. Two quantities have been investigated in detail: the atom number [3,4,6,7,8,9] and the specific heat [5,7,9]. For a finite but large (typically 10^6) number of atoms, the properties of the atomic cloud change abruptly at a characteristic temperature we will name the transition temperature T^* . This temperature is shifted compared to T_c , but by a small amount, typically of few percent for atom numbers around 10^6 . There is also a characteristic temperature for the specific heat; it is different from the previous one but still close to T_c [5,9].

Surprisingly, less attention has been paid on the atomic density of an ideal gas [10]. In a homogeneous gas it is obviously equivalent to the atom number but this is no more the case in a spatially varying potential. It becomes the good parameter of the theory, in particular to perform

local density approximations. This quantity is then particularly important for the study of the shift of the critical temperature by the interatomic interactions, both within the mean-field approximation [6] and beyond this approximation [11]. We will show, in the case of an isotropic harmonic trapping and for a finite atom number, that the ground-state density at the centre of the trap increases much more sharply than its population as the temperature decreases. This leads to the fact that near the Bose-Einstein transition temperature the density is already dominated by the ground-state contribution. This holds whatever the atom number is, and is a remanence of the infinite compressibility of an ideal gas at the thermodynamic limit [12]. Usual semi-classical approximations do not take into account the ground-state contribution and then fail in the vicinity of the Bose-Einstein transition temperature. This is not a finite size effect in the sense that it is not related to the discretization of the excited states energy levels. We will compare the exact results with semi-classical approximations. The addition of the ground-state contribution on the latter ones improves their accuracy. We will finally show that the influence of the ground-state is smaller if the measured quantity is the density integrated over at least one dimension. It is still large for typical experimental parameters.

We will perform our calculations in the grand canonical ensemble (GCE). Then, the Bose-Einstein distribution gives the population N_i of a given energy level ϵ_i : $N_i = (e^{\beta(\epsilon_i - \mu)} - 1)^{-1}$ with $\sum_{i=0}^{\infty} N_i = N$. Here $\beta = 1/k_B T$

^a Permanent address: Departamento de Física, Universidade do Minho, Campus de Gualtar, 4710-057 Braga, Portugal
Correspondence to: denis.boiron@iota.u-psud.fr

with k_B the Boltzmann's constant, μ the chemical potential and N the total atom number. The equivalence between GCE and the canonical or microcanonical ensemble, these latter being probably more appropriate descriptions, is generally not guaranteed, especially for systems that are not at the thermodynamic limit. For instance, it is well known that the GCE predicts unphysical large fluctuations of the condensate population at low temperature [13]. However, the authors of Ref. [10,14,15] have shown that the occupation numbers N_i in GCE are very close to the ones in the canonical ensemble. The difference is more pronounced for small atom number and anisotropic clouds. As a result and because GCE enables to give analytic expressions on contrary to the other ensembles, we will use GCE in the following.

For a fixed atom number, the chemical potential increases as the temperature decreases. As μ has to be smaller than ϵ_0 , the ground-state energy, the excited states population will saturate when μ approaches ϵ_0 whereas N_0 is still increasing: $N - N_0 = \sum_{i=1}^{\infty} N_i(\mu, T) \leq \sum_{i=1}^{\infty} N_i(\epsilon_0, T)$. As in Ref. [2,16], we will define the transition temperature T^* as the temperature for which the excited states saturated population is equal to the total atom number:

$$\sum_{i=1}^{\infty} N_i(\epsilon_0, T^*) = N \quad (1)$$

As pointed out in the introduction, there is not a unique definition of the transition temperature for a finite atom number. Other definitions use, for instance, a change in the slope for the condensate fraction in function of temperature (more explicitly $\frac{d^3(N_0/N)}{dT^3} = 0$) [17], a change in the power dependence on the condensate fraction in function of the atom number [9], which are also pertinent. We have checked that these various definitions affect marginally the value of T^* and do not modify our conclusions [18]. In the following we will then use Eq.(1) to define T^* . Note that the chemical potential μ^* at the transition temperature is close but not equal to the ground-state energy; it is determined by the constraint

$$\sum_{i=0}^{\infty} N_i(\mu^*, T^*) = N \quad (2)$$

There are only a few examples of trapping potentials where the eigen-energies and the eigen-functions are known exactly. Semi-classical approximations give usually accurate enough results and are suited to include interatomic interactions, at least perturbatively. We will derive various type of semi-classical approximations in the following and test their accuracy because the harmonic potential is an exactly solvable potential.

We will first examine the situation where $\hbar\omega \ll k_B T$ with ω the oscillation frequency of the isotropic harmonic trap. This corresponds to the large atom number limit and semi-classical approximations should work. Replacing the discrete energy spectrum by a continuous one and neglecting the ground-state energy ϵ_0 , the density is

$\rho(r) = \frac{1}{\lambda^3} g_{\frac{3}{2}}[z \exp(-\frac{\tau}{2}(r/\sigma)^2)]$ with $z = e^{\beta\mu}$ the fugacity, $\tau = \frac{\hbar\omega}{k_B T}$ and $g_{\frac{3}{2}}(\cdot)$ a Bose function [19]. With the above notation, the thermal de Broglie wavelength is $\lambda = \sigma\sqrt{2\pi\tau}$ and the size of the cloud is $\sqrt{\frac{k_B T}{m\omega^2}} = \sigma/\sqrt{\tau}$. Similarly, the atom number is $N = g_3(z)/\tau^3$. Equation (1) leads then to $N = \zeta(3)/\tau^{*3}$, with τ^* the value of τ at $T = T^*$. The above expressions for the density and atom number are in fact approximations for the excited states and do not contain the ground-state contribution. Then μ^* defined by Eq.(2) is equal to 0 and $z^* = 1$. The transition temperature defined here corresponds to the critical temperature T_c . The peak density at the transition temperature is then given by $\rho(0)\lambda^3 = g_{\frac{3}{2}}(z^*) = \zeta(3/2) \approx 2.612$. For temperatures below T_c , the excited states population is given by $\zeta(3)/\tau^3$. Then, the ground-state population fraction is $N_0/N = 0$ for $T > T_c$ and $N_0/N = 1 - (T/T_c)^3$ for $T < T_c$. This fraction will be plotted in fig.1, labelled with sc_{∞} .

These approximations are too crude and give inaccurate results for the atomic density, however. The reason is that the ground-state contribution cannot be neglected. A better expression is $\rho(r) = \frac{1}{\lambda^3} g_{\frac{3}{2}}[z e^{-\frac{\tau}{2}(r/\sigma)^2}] + \rho_0(r)$ and similarly $N = \frac{1}{\tau^3} g_3(z) + N_0$ with $\rho_0(r) = \frac{N_0}{(\sqrt{\pi}\sigma)^3} e^{-(r/\sigma)^2}$ and $N_0 = \frac{z}{1-z}$. The value of T^* is unchanged as it is defined by the excited states saturation, but z^* is now different from 1. Using $g_3(z^*) \approx \zeta(3) - \zeta(2)x^*$ with $z^* = e^{-x^*}$ ($x = \beta(\epsilon_0 - \mu) > 0$), one finds using Eq.(2) that $x^* \approx \tau^{*3/2}/\sqrt{\zeta(2)}$ [9]. The ground-state population is $\sim 1/x^*$ and, as expected, is vanishingly small as $\tau^* \rightarrow 0$ compared to the excited-state population $\zeta(3)/\tau^{*3}$. The ground-state peak density is $\sim \frac{1}{(\sqrt{\pi}\sigma)^3 x^*}$ whereas the excited state peak density is $\zeta(3/2)/\lambda^{*3}$. As $\lambda^* = \sigma\sqrt{2\pi\tau^*}$, the two quantities have the same order of magnitude! The above high-N analysis predicts then that the degeneracy parameter at the transition temperature is $\rho(0)\lambda^3 = \zeta(3/2) + 2\sqrt{2\zeta(2)} \approx 6.24$ and not 2.612. The ground-state population is extremely small but the size of its wavefunction is also extremely small compared to the atomic cloud size. For a harmonic trap both depend on the same small parameter, raised to the same power. So, even for very large atom number, the traditional criterion for BEC should be modified. This effect is linked to the pathological behaviour of the ground-state density at the thermodynamic limit, i.e. the infinite compressibility of an ideal gas [12]. This limit means $N \rightarrow \infty$ with $N\omega^3 \rightarrow \text{constant}$. The ground-state size being $\sigma = \sqrt{\hbar/m\omega}$, the density of that state behaves as \sqrt{N} below threshold and is then infinite at the thermodynamic limit whereas the density above T_c is finite.

We will now address the case of atom numbers in the accessible experimental range, $10^3 - 10^6$. It is well known that the transition temperature will be shifted compared to T_c [3,4,7]. A better approximation, which takes into account the ground-state energy to first order, is $\rho(r) = \frac{1}{\lambda^3} \{g_{\frac{3}{2}}[\tilde{z}(r)] + \frac{3\tau}{2} g_{\frac{1}{2}}[\tilde{z}(r)]\}$ where $\tilde{z}(r) = z e^{-\frac{\tau}{2}(r/\sigma)^2}$. Then $N = \frac{1}{\tau^3} [g_3(z) + \frac{3\tau}{2} g_2(z)]$. The corresponding transition

temperature is T_{sc}^* such that $N = \frac{1}{\tau_{sc}^*} [\zeta(3) + \frac{3}{2}\zeta(2)\tau_{sc}^*]$. This is the usual semi-classical approximation found in the literature. The ground-state population fraction is then $N_0/N = 0$ for $T > T_{sc}^*$ and $N_0/N = 1 - (\frac{T}{T_{sc}^*})^3 \frac{\zeta(3) + \frac{3}{2}\tau_{sc}^*\zeta(2)}{\zeta(3) + \frac{3}{2}\tau_{sc}^*\zeta(2)}$ for $T < T_{sc}^*$. This fraction, also plotted in fig.1, will be labelled with sc_0 . Note that $g_{\frac{1}{2}}(z)$ diverges at $z = 1$ [20], meaning that this approximation is intrinsically inaccurate near the centre of the trap and near the transition temperature. This divergence is however weak, and any spatial integration would give a finite result. We can still cure this pathology by adding, as before, the ground-state contribution. We obtain then

$$\begin{cases} \rho_{sc}(r) = \frac{1}{\lambda^3} \{g_{\frac{3}{2}}[\tilde{z}(r)] + \frac{3}{2}\tau_{sc} g_{\frac{1}{2}}[\tilde{z}(r)]\} + \frac{z}{1-z} \frac{e^{-\frac{r}{\sigma}}}{(\sqrt{\pi}\sigma)^3} \\ N = \frac{1}{\tau_{sc}^*} [g_3(z) + \frac{3}{2}\tau_{sc} g_2(z)] + \frac{z}{1-z} \\ T_{sc}^* \text{ such that } N = \frac{1}{\tau_{sc}^*} [\zeta(3) + \frac{3}{2}\zeta(2)\tau_{sc}^*] \end{cases} \quad (3)$$

This semi-classical approximation will be labelled with sc in the following. The comparison of T_{sc}^* with the value given by the exact model (see below) can be used to check the finite size correction. Even so, this comparison is useless to check the contribution coming from the ground state since it does not depend on it (same transition temperature as sc_0).

We can now test these semi-classical approximations for a harmonically trapped gas. As we referred before, for this case, the eigen-energies and the eigen-functions are known exactly. The corresponding expressions of the atomic density and atom number [13], labelled with ex in the following, are :

$$\begin{cases} \rho_{ex}(r) = \frac{1}{(\sqrt{\pi}\sigma)^3} \sum_{l=1}^{\infty} \frac{z^l}{(1-e^{-2\tau l})^{3/2}} e^{-\tanh(\frac{\tau l}{2})(\frac{r}{\sigma})^2} \\ N = \sum_{l=1}^{\infty} \frac{z^l}{(1-e^{-\tau l})^3} \\ T_{ex}^* \text{ such that } N = \sum_{l=1}^{\infty} \left(\frac{1}{(1-e^{-\tau_{ex}^* l})^3} - 1 \right) \end{cases}$$

where, here $z = e^{\beta(\mu - \epsilon_0)}$. The semi-classical model corresponds to a Taylor expansion in τ of these last expressions.

In fig.1 we plot the ground-state population fraction in function of the temperature for the various models described above. When the number of atoms is only 10^3 , finite size effects are large. The prediction of model sc_{∞} is clearly wrong compared to the exact model prediction. On contrary models sc_0 and sc give a result close to the one of ex [21]. Figure 2 shows the relative deviations of T_c and T_{sc}^* from T_{ex}^* in function of the atom number. As expected the different values are similar but, as above, the model sc give a closer result to ex than sc_{∞} . The value T_{sc}^* deviates less than 1% for $N > 400$ and the relative shift is $\sim 10^{-4}$ for typical experimental atom numbers. This is well below actual experimental uncertainties. The thermodynamic value T_c deviates more, typically 1 % but is still close to T_{ex}^* [3,4,7,9]. The discrepancy with T_c would have been more pronounced for an anisotropic trap (see below).

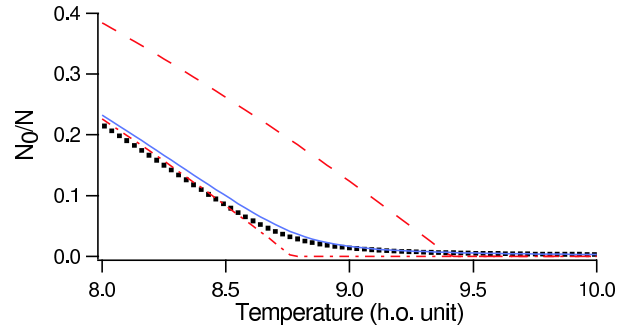


Fig. 1. Ground-state population fraction in function of the temperature in $\hbar\omega/k_B$ unit for a cloud of 10^3 atoms. The dotted curve corresponds to the exact result given by model ex . The solid, dot-dashed and dashed lines correspond respectively to the semi-classical models sc , sc_0 and sc_{∞} . The last two neglect the ground-state contribution above their corresponding transition temperature and the first two take into account finite size effects. The model sc is the closest to ex near Bose-Einstein transition.

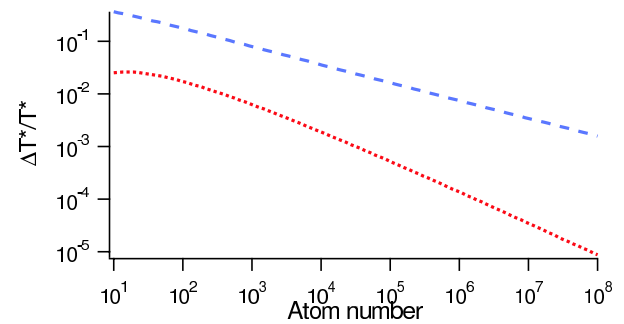


Fig. 2. Relative shift of the semi-classical transition temperatures T_c (dashed line) and T_{sc}^* (dotted line) to T_{ex}^* (see text) in function of the atom number. Both temperatures converge for high atom numbers. The critical temperature at thermodynamic limit, T_c , deviates by less than 1% for $N > 5 \cdot 10^5$. The semi-classical transition temperature defined for a finite atom number, T_{sc}^* , is much more accurate and deviates by less than 1% for $N > 400$.

This two figures illustrate what is called finite size effects, the fact that the energy level spacing is not negligible compared to the temperature. What we are interested in is the role of the ground-state. For this, the transition temperature and the condensate population fraction are not the best observables. It is nevertheless already clear from fig.1 that sc is a significant improved model to describe semi-classically a cloud near degeneracy compared to sc_0 . The high- N model predicts that the ground-state influence should be much more pronounced on the peak density. We will now focus our attention on that observable, only in the more pertinent comparison between the models sc and ex .

This is first illustrated on fig. 3 where the degeneracy parameter $\rho(0)\lambda^3$ is plotted in function of the atom number for clouds at $T = T^*$. We plot this number for the semi-classical approximation sc and for the exact model,

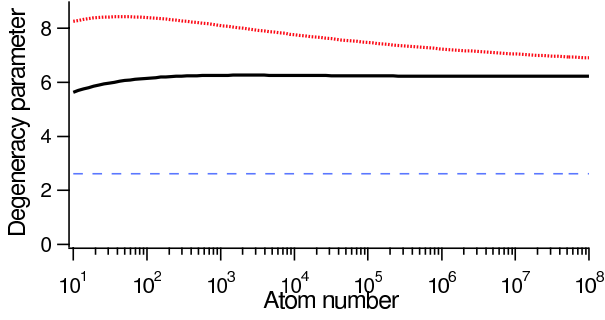


Fig. 3. Degeneracy parameter $\rho(0)\lambda^3$ in function of the atom number N for clouds at the transition temperature. The dotted line corresponds to the semi-classical model sc at $T = T_{sc}^*$ and the solid line to model ex at $T = T_{ex}^*$. Even if the degeneracy parameters are somewhat different, they both differ significantly to the usual value of 2.612 (dashed horizontal line). This deviation is due to an under-estimation of the ground-state density. The actual values are close to our high- N prediction of 6.24 (see text).

ex . The two curves are higher than 2.612. This highlights the inaccuracy of the standard semi-classical models (sc_0 or sc_∞) that do not take into account the ground-state contribution. It confirms also the calculation developed above. The degeneracy parameter is astonishingly constant till 10^3 atoms and does not differ much even for smaller atom numbers. Models sc and ex , which have almost the same transition temperature, have the same asymptotic value of the degeneracy parameter. This value, 6.24, is the one predicted by our high- N analysis. The model sc is significantly higher than this value for experimentally accessible atom numbers. This is because our first analysis does not take into account the $\frac{3}{2}\tau$ term of model sc . To first order [19], $x_{sc}^* \approx \frac{(\tau_{sc}^*)^{\frac{3}{2}}}{\sqrt{\zeta(2)}} (1 + \frac{9}{8\zeta(2)} \tau_{sc}^* \ln \tau_{sc}^*)$ and is then slightly smaller than $\frac{(\tau_{sc}^*)^{\frac{3}{2}}}{\sqrt{\zeta(2)}}$. Consequently the ground-state peak density is bigger at T_{sc}^* using model sc than at T_c using the high- N model. The excited states peak density is also higher in model sc because of this $\frac{3}{2}\tau g_{\frac{1}{2}}$ term.

The next three figures deal with the cloud properties around the Bose-Einstein threshold. Figure 4 and fig.5 show the evolution of the condensate fraction N_0/N and the condensate peak density fraction in function of T for two different atom numbers, 10^6 and 10^3 . Figure 6 shows the density profile of clouds near degeneracy. What prevails in fig.4 is the sharp increase of the condensate peak density compared to the condensate population. Moreover the models sc and ex give very close results validating our analysis on the ground-state contribution near degeneracy. This means that the peak density is a much better marker of the Bose-Einstein threshold than the atom number. This feature is in fact used experimentally: the appearance of a small peak over a broad distribution is the usual criterion to distinguish clouds above or below the transition temperature. This sharpness also explains

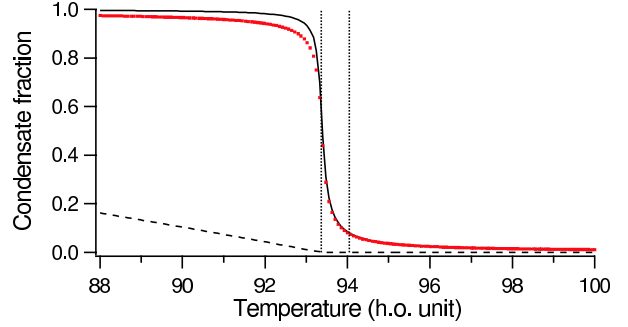


Fig. 4. Condensate atom number fraction N_0/N (dashed line) and peak density fraction $\rho_0(0)/\rho(0)$ (solid line) in function of the temperature in harmonic oscillator unit $\hbar\omega/k_B$, using model ex . The cloud contains 10^6 atoms. The transition temperature is $T_{ex}^* = 93.37\hbar\omega/k_B$ and the asymptotic thermodynamic temperature is $T_c = 94.05\hbar\omega/k_B$. The positions of these temperatures are shown as vertical lines in the figure. The ground-state peak density increases much more sharply than the ground-state population around the transition temperature. The former has also a significant value above T_{ex}^* . The model sc is indistinguishable for N_0/N , but is slightly different for $\rho_0(0)/\rho(0)$ (dotted line).

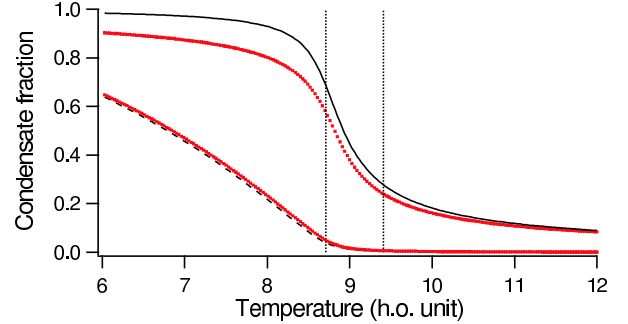


Fig. 5. Same as in Fig.4 but with 10^3 atoms. The transition temperature is $T_{ex}^* = 8.71\hbar\omega/k_B$ and the asymptotic thermodynamic temperature is $T_c = 9.41\hbar\omega/k_B$. Since the number of populated states is considerably reduced compared to fig.4, the discrepancy between sc (dotted lines) and ex is more pronounced. This also explains why the increase of the condensate peak density is slower.

why the value of the peak density is very sensitive to the value of the temperature (cf. fig.3). Figure 4 shows also that, above threshold, the ground-state peak density fraction decays slowly. This is even more pronounced in fig.5 where $N = 10^3$ instead of 10^6 . It comes from the fact that the number of populated states is not macroscopic anymore ($k_B T < 10\hbar\omega$) and then the transition is smoother for smaller atom number. Once again, the density is a better marker of degeneracy than the atom number. This figure shows also that the $\frac{3}{2}\tau$ term and the ground-state contribution make the model sc still very close to model ex , respecting the density and population fractions, even for 10^3 atoms.

The above analysis is focused on the peak density i. e. at the centre of the cloud. Figure 6 shows the total density

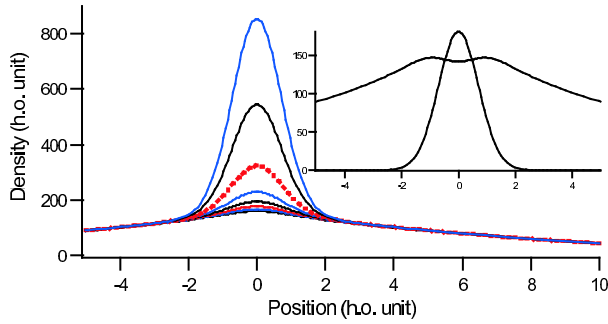


Fig. 6. Atomic density ρ_{ex} in function of r/σ where σ is the size of the harmonic oscillator ground-state. The temperature is $T = 93.37\hbar\omega/k_B$ and the atom number N spans from $0.990 \cdot 10^6$ to $1.004 \cdot 10^6$ by step of 2000 atoms. The curve at threshold is in dotted line and corresponds to 10^6 atoms. The inset shows the excited states and ground state density profile at threshold. The dip around $r = 0$ is mainly due to the first excited state population.

profile of clouds, all at the same temperature, but containing different numbers of atoms around N_{ex}^* , the number of atoms for which $T = T_{ex}^*$ ($N = N_{ex}^*$ corresponds to the dotted line). This figure simulates somehow an experimental observation of BEC threshold. Only the central part is sensitive to the atom number; this corresponds to the condensate growing as the number of atoms is increased and to the fact that the excited states are already saturated for these atom numbers. Moreover, by looking at the graph, one would rather think that the Bose-Einstein transition occurs for a smaller atom number. This points out that the definition on the transition temperature based on an atom number criterion does not fully correspond to the one based on the atomic density which would be more connected to experiments. The inset shows the excited states and ground state density profiles at threshold. The excited states density exhibits a dip in the centre of the cloud, obviously not present in semi-classical models (monotonic functions). We check that the height of the dip is proportional to $1/\tau$ and can almost be totally attributed to the first excited state population. The aim of this paper is to show the importance of the ground-state in the study of non-interacting clouds close to threshold. The inset reveals that the first excited state density is also largely under-estimated; it represents $\sim 10\%$ of the peak density whereas it contributes only to $\sim 0.1\%$ of the population.

We have shown results on the atomic density at the vicinity of the transition temperature. Detection techniques consist rather on 1D-integrated density, corresponding to 2D absorption images, or 2D-integrated density [23]. One can show that, at threshold, the 1D and 2D-integrated peak density of the ground-state are vanishingly small for large atom numbers on contrary to the non-integrated case. The peak 1D-integrated density fraction behaves at threshold as $\sqrt{\tau}$ and the 2D-integrated peak density as τ . For typical atom number this is nevertheless not negligible. This is illustrated in Fig.7 where is plotted the con-

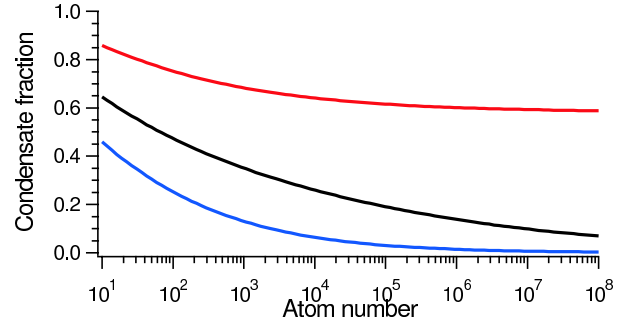


Fig. 7. Contribution of the ground-state on the peak density for, from bottom to top, 1D, 2D and 3D images in function of the number of trapped atoms. The clouds are at the transition temperature T_{ex}^* and the calculations use model *ex*. A 3D image would give the density in all three dimensions of space [25] whereas a 2D (resp. 1D) image corresponds to the density integrated over one (resp. 2) dimension. For $N = 10^4$ atoms the ground-state contributes to $\sim 26\%$ in 2D images and $\sim 6\%$ in 1D images. In contrast to 3D image, the ground-state contribution is very small for large atom number; it is not for typical atom numbers accessible in experiments.

densate peak density fraction for 3D, 2D and 1D images of clouds at threshold. The calculations use the model *ex*. At the transition temperature T_{ex}^* , the ground-state contributes to more than 10% for $N < 2500$ atoms in 1D images and for $N < 8 \cdot 10^6$ atoms for 2D images. It means that, even with the conventional technique of absorption images, the effect should be experimentally observable if interactions could be switched off using, for instance, the magnetic tunability of the scattering length close to a Feshbach resonance [24].

Apart from the atomic density, two- and three-body inelastic loss rates will also be affected and could be 20 to 30 % higher than predicted by model *sc0* around the transition temperature for typical atom numbers. Finally, in most experimental set-ups, the trapping potential is anisotropic and finite size effects are then stronger. Indeed the term $\frac{3}{2}\tau$ in Eq.(3) should be replaced by $\frac{3}{2}\bar{\omega}\tau$, with $\bar{\omega} = (\prod_i \omega_i)^{1/3}$ the geometric mean and $\tilde{\omega} = \frac{1}{3} \sum_i \omega_i$ the arithmetic mean [3]. Whatever the anisotropy is, $\tilde{\omega}$ is always larger than ω , making the finite size contribution stronger. To first order and if $k_B T_{ex}^* \gg \hbar\omega_i$ for $i = x, y$ and z , the ground-state contribution should be the same since our high-N analysis does not depend on any anisotropy.

In conclusion, we have shown that the density of an ideal atomic gas is dominated by the ground-state contribution near the transition temperature. The inter-atomic interactions have been neglected in our analysis and will modify our conclusions. With repulsive interactions, the clouds tends to decrease its density at the centre of the cloud whereas it tends to increase it with attractive interactions. Previous calculations have treated separately finite size and interactions effects, both corrections being finally added [6]. Since the ground-state has a non-perturbative effect on the density, our analysis tends to prove that both effects have to be investigated together.

The approach of Ref.[10] could in this respect provide helpful informations. Feshbach resonances, which enable to tune the interactions strength, constitute a powerful tool to check the accuracy of the different theoretical models. Moreover, a full three-dimensional density measurement would also be valuable; this type of measurement is at the edge to be available in our experiment on metastable helium in Orsay [25].

We thank S. Giorgini for stimulating discussions. The Atom Optics group of LCFIO is member of the Institut Francilien de Recherche sur les Atomes Froids (IFRAF).

References

1. Proceedings of the International School of Physics "Enrico Fermi", Course CXL, edited by M. Inguscio, S. Stringari, C. E. Wieman, IOS Press, Amsterdam (1999).
2. F. Dalfovo, S. Giorgini, L. P. Pitaevskii, S. Stringari, *Rev. Mod. Phys.* **71**, 463 (1999).
3. S. Grossmann and M. Holthaus, *Z. Naturforsch. Teil A* **50**, 921 (1995).
4. W. Ketterle and N. J. van Druten, *Phys. Rev. A* **54**, 656 (1996).
5. K. Kirsten and D. J. Toms, *Phys. Rev. A* **54**, 4188 (1996).
6. S. Giorgini, L. P. Pitaevskii and S. Stringari, *Phys. Rev. A* **54**, R4633 (1996).
7. H. Haugerud, T. Haugest and F. Ravndal, *Phys. Lett. A* **225**, 18 (1997).
8. S. Giorgini, L. P. Pitaevskii and S. Stringari, *J. Low Temp. Phys.* **109**, 309 (1997).
9. R. K. Pathria, *Phys. Rev. A* **58**, 1490 (1998).
10. W. Krauth, *Phys. Rev. Lett.* **77**, 3695 (1996).
11. P. Arnold and B. Tomášik, *Phys. Rev. A* **64**, 053609 (2001).
12. K. Huang, *Statistical Mechanics*, Wiley ((1987).
13. L. D. Landau and E. M. Lifshiz, *Statistical Physics*, Butterworths (1996).
14. H. D. Politzer, *Phys. Rev. A* **54**, 5048 (1996).
15. C. Herzog and M. Olshanii, *Phys. Rev. A* **55**, 3254 (1997).
16. Y. Castin, lecture note in "Coherent atomic matter waves", Les Houches Session LXXII, eds. R. Kaiser, C. I. Westbrook and F. David, Springer (2001).
17. T. Bergeman, D. L. Feder, N. L. Balazs, B. I. Schneider, *Phys. Rev. A* **61**, 063605 (2000).
18. In Ref.[9], the transition temperature was indeed T_{sc} (see later in the text). The transition temperature defined by the maximum of the second derivative of the condensate fraction has been calculated for atom number in the range $10^3 - 10^8$; the relative deviation is below $\sim 10^{-3}$ on the transition temperature and $\sim 10^{-2}$ on the condensate peak density fraction.
19. We use the usual definition of Bose functions $g_a(x) = \sum_{l=1}^{\infty} x^l/l^a$. We remind that $g_a(1) = \zeta(a)$ with $\zeta()$ the Riemann Zeta function. Note that $g_1(x) = -\ln(1-x)$ and $\frac{dg_a}{dx}(x) = g_{a-1}(x)/x$.
20. After submission of this article, we have been aware of a different type of semi-classical approximations which does not give rise to divergences. See V. I. Yukalov, *Phys. Rev. A* **72**, 033608 (2205).
21. We use the result of Ref. [22] for the calculation of the Bose functions near the transition temperature. For the series in model ex , the convergence is very slow but can easily be accelerated. For instance, it is much better to write $N = \frac{z}{1-z} + \sum_{l=1}^{\infty} z^l (\frac{1}{1-e^{-\tau l}} - 1)$ because the second term converges for large l because of the z^l part and because of the $(\frac{1}{1-e^{-\tau l}} - 1)$ part.
22. J. E. Robinson, *Phys. Rev.* **83**, 678 (1951).
23. A. Robert, O. Sirjean, A. Browaeys, J. Poupard, S. Nowak, D. Boiron, C. I. Westbrook, and A. Aspect, *Science* **292**, 461 (2001); published online 22 march 2001 (10.1126/science.1060622).
24. V. Vuletic, A. J. Kerman, C. Chin, S. Chu, *Phys. Rev. Lett.* **82**, 1406 (1999).
25. M. Schellekens, R. Hoppeler, A. Perrin, J. Viana Gomes, D. Boiron, A. Aspect, and C. I. Westbrook, *Science* **310**, 648 (2005); published online 15 september 2005 (10.1126/science.1118024).